J|A|C|S
COMMUNICATIONS

Published on Web 05/23/2007

An Unprecedented $Fe^{III}(\mu\text{-OH})Zn^{II}$ Complex that Mimics the Structural and Functional Properties of Purple Acid Phosphatases

Ademir Neves,*[,†] Mauricio Lanznaster,[†] Adailton J. Bortoluzzi,[†] Rosely A. Peralta,[†] Annelise Casellato,[†,§] Eduardo Ernesto Castellano,[‡] Paul Herrald,[§] Mark J. Riley,[§] and Gerhard Schenk[§]

LABINC, Departamento de Química, Universidade Federal de Santa Catarina, 88040-900 Florianópolis, SC, Brazil, Instituto de Física, Universidade de São Paulo, 13560-970 São Carlos, SP, Brazil, and School of Molecular and Microbial Sciences, The University of Queensland, St. Lucia, QLD 4072, Australia

Received February 18, 2007; E-mail: ademir@qmc.ufsc.br

Purple acid phosphatases (PAPs) belong to the family of binuclear metallohydrolases and catalyze the hydrolysis of a variety of phosphoester substrates within the pH range of 4−7.[1] They are the only binuclear metallohydrolases where the necessity for a heterovalent active site ($Fe^{III}-M^{II}$, where M = Fe, Zn, or Mn) for catalysis has been clearly established. To date, the crystal structures of PAPs from red kidney bean (rkbPAP),[2a] rat,[2b,c] pig,[2d] human,[2e] and sweet potato[2f] have been reported. In the structure of rkbPAP,[2a] the Fe^{III} ion is coordinated by a tyrosine, a histidine, and an aspartate, and a Zn^{II} ion is coordinated by two histidines and an asparagine. The $Fe^{III}Zn^{II}$ ions are bridged by two oxygen atoms, one from the carboxylate group of an aspartate and the other from a modeled μ-(hydr)oxo group. Two oxygen atoms from a μ-1,3 phosphate group complete the coordination spheres of the Zn^{II} and Fe^{III} ions.

Despite the availability of detailed structural data, the catalytic mechanism of PAPs remains a matter of controversy. For rkbPAP, a mechanism in which, in the first step of the catalytic cycle, the substrate binds in a monodentate fashion to the Zn^{II} ion has been proposed.[2a] The enzyme−substrate complex is oriented in such a way that a terminal Fe^{III}-bound hydroxide can efficiently attack the phosphorus atom of the substrate, leading to the release of the alcohol product.[2a] The monodentate binding of the substrate to Zn^{II} is corroborated by the fact that the addition of phosphate to the $Fe^{III}Zn^{II}$ derivative of bovine spleen PAP does not affect the spectroscopic properties of the Fe^{III} ion at the pH of optimal activity (pH 6.5).[3] However, for pig[4a] and sweet potato PAP,[2f,4b] an alternative mechanism in which the substrate forms a μ-1,3 phosphate complex, thus placing the μ-(hydr)oxo bridge in an ideal position to act as the reaction-initiating nucleophile, has also been proposed.

Homo- and heterodinuclear $Fe^{III}M^{II}$ complexes which are capable of reproducing the structural, spectroscopic, and functional properties of PAPs can be very informative to evaluate the mechanism(s) of these metalloenzymes. Recently, we reported on the syntheses, characterization, and phosphatase-like activity of the heterodinuclear $[LFe^{III}(\mu\text{-OAc})_2Zn^{II}]^+$ complex (H_2L = 2-bis[{(2-pyridylmethyl)-aminomethyl}-6-{(2-hydroxybenzyl)-(2-pyridylmethyl)}aminomethyl]-4-methylphenol), and we have proposed that upon dissolving the complex in an aqueous solution the dissociation of the carboxylate groups leads to the formation of the catalytically active $[(OH)Fe^{III}-(\mu\text{-OH})Zn^{II}(OH_2)]$ species,[5] similar to that proposed to be present in the active site of rkbPAP.[2a] Herein we report the X-ray structure, solution studies, and phosphatase activity of the first mixed-valence

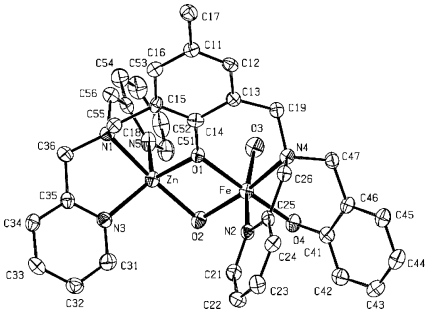

Figure 1. ORTEP plot of the cation in **1**.

complex containing the $Fe^{III}(\mu\text{-OH})Zn^{II}$ motif (**1**). The molecular structure of **1** (Figure 1) shows that in the dinuclear $[L(OH_2)Fe-(\mu\text{-OH})Zn]^{2+}$ unit the Fe^{III} ion is facially coordinated by the hard tridentate pendant arm of L^{2-} containing the amine (N4) and pyridine nitrogen (N2) and the phenolate oxygen (O4) atoms, while Zn^{II} is coordinated by the soft side of L^{2-} through the amine (N1) and pyridine (N3, N5) nitrogen atoms. The bridging phenolate oxygen O1, the bridging hydroxo group (O2), and a terminal water molecule (O3) complete the octahedral N_2O_4 coordination of Fe^{III}, while the distorted trigonal bipyramid of Zn^{II} is complemented by the bridging phenolate (O1) and the hydroxo (O2) oxygen atoms. The Fe−μ-OH and Zn−μ-OH distances in **1** are 1.934(6) and 1.966-(5) Å, respectively, which are somewhat shorter than the corresponding metal−OH distances in rkbPAP, which have been modeled between 2.0 and 2.2 Å.[2a] Furthermore, the $Fe^{III}\cdots Zn^{II}$ distance of 3.040(1) Å in **1** is shorter but comparable to the 3.20 Å found in rkbPAP. Importantly, the structure of **1** reveals the presence of a terminal Fe-bound water molecule (Fe−O3 = 2.054(6) Å), which occupies a position equivalent to that of the proposed nucleophile in rkbPAP (vide supra).[2a]

Potentiometric titration of **1** in water/CH_3CN (50:50) showed the neutralization of 3 mol of KOH/mol of complex in the pH range of 2−10. Fitting the data with the BEST7 program (Figure S1) resulted in the following deprotonation constants: pK_{a1} = 2.93, pK_{a2} = 4.81, and pK_{a3} = 8.30. These pK_a values are consistent with the following equilibria: $[(OH_2)Fe(\mu\text{-}OH_2)Zn(OH_2)]$(**a**) ↔ $[(OH_2)Fe(\mu\text{-OH})Zn(OH_2)]$(**b**) ↔ $[(OH)Fe(\mu\text{-OH})Zn(OH_2)]$(**c**) ↔ $[(OH)Fe(\mu\text{-OH})Zn(OH)]$(**d**). Species **b** is the one determined by X-ray crystallography, with an additional Zn-coordinated water molecule. The solution structure of **1** was further investigated using X-ray absorption fine structure (XAFS) spectroscopy. The comparison of the 10 K solid state and (frozen) solution Fe and Zn XAFS data indicates that both metal centers are six-coordinate in solution (Figure S2). Importantly, a Fe···Zn distance of ∼3.04 Å is found, in full agreement with the X-ray structure of **1** (see above)

† Universidade Federal de Santa Catarina.
‡ Universidade de São Paulo.
§ The University of Queensland.

10.1021/ja071184l CCC: $37.00

and indicating the retention of the μ-OH bridge in solution. This hypothesis is supported by the lack of intensity change in the Fe pre-edge features in going from solid to solution, indicating that the centrosymmetric environment is maintained.[6]

The phosphatase-like activity of **1** was determined using the activated substrate 2,4-bis(dinitrophenyl)phosphate (BDNPP) by following spectrophotometrically the absorbance increase of the liberated 2,4-dinitrophenolate anion (λ_{max} = 400 nm), under conditions of excess substrate. The ability of **1** to cleave BDNPP is strongly influenced by the pH of the reaction mixture with a bell-shaped pH rate profile (Figure S3) and an optimum at pH 6.5, which is similar to that found for rkbPAP.[2a] Sigmoidal fits reveal pK_a values of 5.3 and 8.1. which are in good agreement with the pK_{a2} = 4.81 and pK_{a3} = 8.30 obtained from the potentiometric titration experiments, demonstrating that the catalytically active species is of the type [(OH)Fe(μ-OH)Zn(OH$_2$)]. The pK_a value of 5.3 obtained from the acid limb of the V_0 versus pH profile is due to the protonation equilibrium in the catalyst−substrate complex, while the corresponding pK_{a2} of 4.81 is associated with the free catalyst. The determination of the initial rates at pH 6.5 as a function of substrate concentration reveals saturation kinetics with Michaelis−Menten-like behavior (Figure S4). The kinetic parameters (k_{cat} = 9.13 × 10^{-4} s^{-1} and K_M = 4.20 × 10^{-3} mol L^{-1}) were obtained after Lineweaver−Burk linearization of the initial rates (V_0 vs [BDNPP]; Figure S4). Compared to the uncatalyzed reaction **1** accelerates the turnover rate 4.8 × 10^3-fold. Furthermore, the measured kinetic isotope effect of k_H/k_D = 1.34 (Figure S5) suggests that no proton transfer is involved in the rate-limiting step and thus supports an intramolecular nucleophilic attack by an Fe^{III}-bound hydroxide.

In order to elucidate the mode of interaction between BDNPP and the dinuclear catalytic center in **1**, we followed the spectral change of the reaction mixture at the optimum pH over a period of 24 h in the presence of excess substrate (Figure S6). The absorption maximum (λ_{max} = 486 nm) and the intensity of the phenolate−Fe^{III} charge-transfer band are only slightly affected, thus strongly suggesting monodentate binding of the substrate to the Zn^{II}. This hypothesis is strongly supported by EPR spectroscopic data of **1**, measured in the absence and presence of BDNPP (Figure S7), which indicate that the substrate does not interact with the Fe^{III} center. On the other hand, the absorption at 400 nm continues to increase (Figure S6) due to the formation of the product 2,4-dinitrophenolate, with 182 turnovers in 24 h. Interestingly, after 2 weeks at room temperature, a crystal suitable for X-ray diffraction was formed in this solution. The crystal structure (Figure S8) of this complex (**2**) reveals a tetranuclear cation in which two dinuclear {LFe^{III}Zn^{II}} structural units without the OH$^-$ bridge are linked through a phosphate anion. The Zn^{II} is pentacoordinated, while the hexacoordination around Fe^{III} is completed by a 2,4-dinitrophenolate anion. Therefore, a second sequential reaction must be taken into account in which the product of the first reaction cycle, the 2,4-dinitrophenylphosphate (DNPP) monoester, is further hydrolyzed. We tested the activity of **1** for the hydrolysis of the monoester DNPP directly with an excess of substrate, and over a period of ~5 h, only the background reaction was observed. After this time, BDNPP was added to the reaction mixture and immediately the absorbance at 400 nm started to increase (Figure S9), indicating the recovery of the catalyst and hydrolysis of the diester substrate. The coordination of DNPP bridging both metal ions is proposed based on the hypsochromic shift observed after ligation of DNPP to **1**. Therefore, we may conclude that the μ-hydroxide is a significantly poorer nucleophile than the terminally Fe^{III}-bound OH$^-$ group, and that hydrolysis of the monoester to form inorganic phosphate and 2,4-dinitrophenolate occurs exclusively due to the background reaction.

Scheme 1

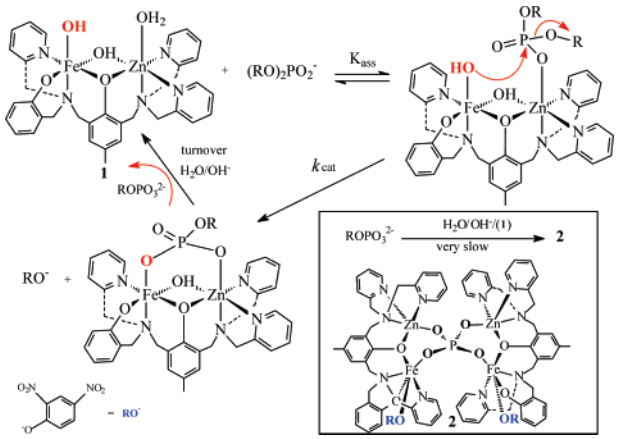

In summary, the combined data support a mechanistic model whereby the [(OH)Fe(μ-OH)Zn(OH$_2$)] species of **1** is the catalytically relevant system (Scheme 1).

In brief, monodentate binding of the substrate to Zn^{II} (K_{ass}) is followed by a nucleophilic attack by the terminal, Fe^{III}-bound hydroxide and the concomitant release of 2,4-dinitrophenolate. The μ-1,3-coordinated DNPP intermediate undergoes substitution by two water molecules and regenerates the active site for the next catalytic cycle. Additionally, in a significantly slower reaction, some of the complex dimerizes to the stable tetranuclear end product (inset in Scheme 1). Further studies involving the synthesis of substituted phenolate−R (R = Me, NO$_2$, Br) derivatives of **1** and their interactions with phosphodiester bonds in model substrates and DNA are underway and will be the subject of future reports.

Acknowledgment. This paper is dedicated to Prof. Faruk Nome. Financial support was received from CNPq and FAPESC (Brazil), the Australian Research Council (DP0558652), and the Australian Synchrotron Research Program.

Supporting Information Available: Crystallographic data of **1** and **2** have been deposited at the Cambridge Structural Database CCDC 637120 and CCDC 637121. Synthesis and characterization for **1** and Figures S1−S9 in PDF format. This material is available free of charge via the Internet at http://pubs.acs.org.

References

(1) Mitić, N.; Smith, S. J.; Neves, A.; Guddat, L. W.; Gahan, L. R.; Schenk, G. *Chem. Rev.* **2006**, *106*, 3338.
(2) (a) Klabunde, T.; Sträter, N.; Fröhlich, R.; Witzel, H.; Krebs, B. *J. Mol. Biol.* **1996**, *259*, 737. (b) Uppenberg, J.; Lindqvist, F.; Svensson, C.; Ek-Rylander, B.; Anderson, G. *J. Mol. Biol.* **1999**, *290*, 201. (c) Lindqvist, Y.; Johansson, E.; Kaija, H.; Vihko, P.; Schneider, G. *J. Mol. Biol.* **1999**, *291*, 135. (d) Guddat, L. W.; McAlpine, A. S.; Hume, D.; Hamilton, S.; Jersey, J.; Martin, J. L. *Structure* **1999**, *7*, 757. (e) Sträter, N.; Jasper, B.; Scholte, M.; Krebs, B.; Duff, A. P.; Langley, D. B.; Han, R.; Averill, B. A.; Freeman, H. C.; Guss, J. M. *J. Mol. Biol.* **2005**, *351*, 233. (f) Schenk, G.; Gahan, L. R.; Carrington, L. E.; Mitić, N.; Valizadeh, M.; Hamilton, S. E.; de Jersey, J.; Guddat, L. W. *Proc. Natl. Acad. Sci. U.S.A.* **2005**, *102*, 273.
(3) Merx, M.; Pinske, M. W. H.; Averill, B. A. *Biochemistry* **1999**, *38*, 9914.
(4) (a) Smoukov, S. K.; Quaroni, L.; Wang, X.; Doan, P. E.; Hoffman, B. M.; Que, L., Jr. *J. Am. Chem. Soc.* **2002**, *124*, 2595. (b) Schenk, G.; Boutchard, C. L.; Carrington, L. E.; Noble, C. J.; Moubaraki, B.; Murray, K. S.; de Jersey, J.; Hanson, G. R.; Hamilton, S. E. *J. Biol. Chem.* **2001**, *276*, 19084.
(5) Lanznaster, M.; Neves, A.; Bortoluzzi, A. J.; Szpoganicz, B.; Schwingel, E. *Inorg. Chem.* **2002**, *41*, 5641.
(6) Lanznaster, M.; Neves, A.; Bortoluzzi, A. J.; Aires, V. V. E.; Szpoganicz, B.; Terenzi, H; Severino, P. C.; Fuller, J. M.; Drew, S. C.; Gahan, L. R.; Hanson, G. R.; Riley, M. J.; Schenk, G. *J. Biol. Inorg. Chem.* **2005**, *10*, 319.

JA071184L